ISSN 1070-3632, Russian Journal of General Chemistry, 2015, Vol. 85, No. 7, pp. 1734–1744. © Pleiades Publishing, Ltd., 2015.

Synthesis, Spectroscopic, Thermal Analyses, and Anti-Cancer Studies of Metalloantibiotic Complexes of Ca(II), Zn(II), Pt(II), Pd(II), and Au(III) with Albendazole Drug[1]

F. A. I. Al-Khodir[a,b] and M. S. Refat[c,d]

[a] *Department of Chemistry, College of Science, Princess Nora Bint Abdul Rahman University, Riyadh, Saudi Arabia*

[b] *Deanship of Scientific Research, Princess Nora Bint Adul Rahman University, Riyadh, Saudi Arabia*

[c] *Department of Chemistry, Faculty of Science, Port Said University, Port Said, Egypt*

[d] *Department of Chemistry, Faculty of Science, Taif University, Al-Hawiah, Taif, P.O. Box 888, Zip Code 21974, Saudi Arabia*
e-mail: msrefat@yahoo.com

Received April 6, 2015

Abstract—This paper presents synthesis, characterization, computational and biological (anti-bacterial, anti-fugal, and anti-cancer) assessment studies of vital metal ions [Ca(II), Zn(II), Pt(II), Pd(II), and Au(III)] complexes of albendazole (Alb). Structures of the titled complexes cited herein were elucidated using elemental analysis, IR, Raman, ^{1}H and ^{13}C NMR, and electronic spectra. The results indicated formation of albendazole complexes by three fashions and albendazole reaction as a bidentate ligand bound to Ca(II), Zn(II), Pd(II), and Au(III) ions via the carbamide oxygen and/or benzimidazole nitrogen. Pt(II) ions coordinated with albendazole ligand via deprotonated benzimidazole ring. The molar conductance measurements confirmed non-electrolyte nature of 1 : 1 metal : ligand (Alb) complexes of Ca(II), Zn(II), and Au(II) and 1 : 2 complexes of Pt(II) and Pd(II). Thus, the complexes could be presented as $[Ca^{II}(Alb)^{0}(Cl)_2(H_2O)_2]$, $[Zn^{II}(Alb)^{0}(Cl)_2]$, $[Pt^{II}(Alb)_2^{2-}(H_2O)_2]$, $[Pd^{II}(Alb)_2^{2-}]$, and $[Au^{III}(Alb)^{-}(Cl)_2]$. Based on the Coats–Redfern and Horowitz–Metzeger methods the kinetic thermodynamic parameters of thermal decomposition have been deduced. The narrow size distribution in nano-scale range for the albendazole complexes is discussed using X-ray powder diffraction (XRD), scanning electron microscopy (SEM), X-ray energy dispersive spectrometery (EDX), and transmission electron microscopy (TEM). Computational studies data for the synthesized complexes are considered.

Keywords: metalloantibiotics, albendazole, metal ions, complexation, anticancer, nano-scale

DOI: 10.1134/S1070363215070270

INTRODUCTION

Interaction among different metal ions and antibiotic drugs is an interesting subject of bioinorganic chemistry due to metalloantibiotics reactions with DNA, RNA, proteins, and lipids. Antibiotics metal complexes were found to be more efficient in chemotherapy than their parent antibiotics [1]. Although most antibiotics do not need metal ions for their biological activity, there is a number of those called metalloantibiotics [2] that exhibit enhanced biological activity [3]. Some metal complexes exhibited remarkable antitumour, antifungal, antiviral, and other biological activities [1, 4–10].

Methyl [5-(propylthio)-1*H*-benzimidazole-2-yl] carbamate, commonly named as albendazole (Alb; Fig. 1) demonstrated the effect of antihelmintic drug [11] efficient against pinworm and whip-worm infections. Albendazole is also used for treatment of lumbricosis, hookworm disease, strongyloidosis, and pork tapeworm infection, and mixed infections caused by those organisms. Albendazole therapy is very important in treating systemic cestode infections especially in inoperable or disseminated cases of hydatidosis [12] and neurocysticercosis [13]. Benzimidazole is essential structural block of organic compounds used as

[1] The text was submitted by the authors in English.

antimicrobial agents against most microorganisms [14–19]. It is important in synthesis of anti-fungal [20], anti-tubercular [21], anti-oxidant [22], anti-allergic [23], antiparasitic [24] and herbicidal [25], anthelmintic [26], nematodes, hidatidosis, and teniasis [27] agents and many other biologically active compounds [28–30]. Cu(II) complexes of benzimidazoles demonstrated antibacterial activity against *S. epidermidis* [31] and fungi [32–36]. Some Pt(II) complexes bearing benzimidazole ligands exhibited mutagenic activity on the RD Rhabdomyosarcoma cell line [37]. Benzimidazole derived drugs have received much attention owing to the fact that benzimidazole moiety is a component of vitamin B_{12} structure [38, 39].

In continuation of our research [40–45] devoted to synthesis, characterization of new metal-drug complexes and their biological assessments, the present study targeted synthesis, characterization, theoretical calculations and biological evaluation of vital metal ions Ca(II), Zn(II), Pt(II), Pd(II), and Au(III) complexes with albendazole antibiotic drug. The experimental studies have been accompanied by theoretical calculations (PM3).

EXPERIMENTAL

Chemicals. Albendazole was received from Aldrich chemical company. All chemicals used in this study were of analytically reagent grade, commercially available from BDH and used without preliminary purification.

Synthesis. Ca(II), Zn(II), Pd(II), and Au(II) albendazole complexes were prepared by refluxing of the mixture of Alb ligand (1 mmol) with one of metal chlorides (1 : 1 molar ratio) in methanol medium on a hotplate for 3–4 h at 60–70ºC. The precipitate was filtered off, washed with methanol and diethyl ether and finally dried in a vacuum desiccator over anhydrous $CaCl_2{\cdot}Pt(Alb)_2(H_2O)_2$ complex was synthesized by dissolving 1 mmol of $K_2(PtCl_4)$ in 10 mL of deionized water to which was added 0.5 g of KI and 1 mmol of Alb upon continuous stirring for 3 h and following reflux at 60–70ºC. The yellowish brown precipitate of Pt(II) complex was filtered off, washed with cold water and ethanol and air dried. Yields of the final products were 60–75%.

Instruments. CHN analyses was carried out in Vario EL Fab. CHNS anlyzer. The amount of water and the metal content were determined by gravimetric analysis. IR spectra of albendazole complexes were recorded on a Bruker infrared spectrophotometer in the range of 400–4000 cm^{-1}. Raman spectra were measured on a Bruker FT-Raman with laser 50 mW. The molar conductances of 10^{-3} M solutions of the complexes in DMSO were measured on a HACH conductivity meter. All measurements were taken at room temperature for freshly prepared solutions. Electronic spectra of the complexes were measured in DMSO with concentration 1×10^{-3} M, in rang 200–800 nm by using Unicam UV/Vis spectrophotometer. Magnetic susceptibility (X_g) of complexes was measured at room temperature using Gouy's method by a magnetic susceptibility balance (Johnson Metthey and Sherwood model) [46]. The effective magnetic moment (μ_{eff}) value was obtained using the following equations (1)–(3) [46].

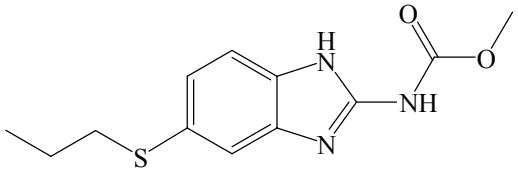

Fig. 1. Structure of albendazole.

$$X_g = \frac{C_{Bal}L(R - R_0)}{M \times 10^9}, \quad (1)$$

$$X_M = X_g x \mathrm{M}Wt, \quad (2)$$

$$\mu_{eff} = 2.84\sqrt{X_M xT}. \quad (3)$$

Here (R_0) reading of empty tube; (L) sample length, cm; (M) sample mass, gm; R reading for tube with sample; (C_{Bal}) balance calibration constant = 2.086. Values of X_M as calculated from Eq. (2) were corrected for the diamagnetism of the ligand using Pascal's constants, and then applied in Curie's equation (3).

^{1}H and ^{13}C NMR spectra were recorded as DMSO solutions on a Bruker 600 MHz spectrometer using TMS as the internal standard. Thermogravimetric analysis (TGA) experiments were conducted using a Shimadzu TGA-50H thermal analyzers. All experiments were performed using a single loose top loading platinum sample pan under nitrogen atmosphere at a flow rate of 30 mL/min and a 10°C/min heating rate for the temperature range 25–800°C. SEM images were obtained using a Jeol Jem-1200 EX II Electron microscope at an acceleration voltage of 25 kV. X-ray diffraction (XRD) patterns of the samples were recorded on X Pert Philips X-ray diffractometer. All

Table 1. Physicochemical data of Alb drug ligand and their metal complexes

Empirical formula	Color	mp, °C	Λ_m, μs	Elemental analysis, % found (calculated)				
				C	H	N	Cl	M
Alb	White	214	5.32	–	–	–	–	–
$[Ca(Alb)(Cl)_2(H_2O)_2]\cdot 2H_2O$	White	>250	6.21	32.27 (32.14)	5.69 (5.17)	9.68 (9.37)	15.55 (15.81)	8.79 (8.94)
$[Zn(Alb)(Cl)_2]$	White	>250	8.21	36.29 (35.89)	4.10 (3.76)	10.55 (10.46)	17.21 (17.65)	15.84 (16.28)
$[Pt(Alb)_2(H_2O)_2]$	Yellowish brown	>250	3.12	36.40 (37.94)	4.45 (4.25)	10.59 (11.06)	–	25.11 (25.68)
$[Pd(Alb)_2]$	Yellowish green	>250	2.22	45.63 (45.39)	5.08 (4.44)	13.25 (13.23)	–	16.43 (16.76)
$[Au(Alb)(Cl)_2]$	Light green	>250	9.21	27.00 (27.08)	2.90 (2.65)	6.98 (7.90)	13.11 (13.32)	36.44 (37.01)

diffraction patterns were obtained by using Cu$K_{\alpha 1}$ radiation, with a graphite monochromator at 0.02 deg/min scanning rate. Transmission electron microscopy was performed with JEOL 100s microscopy.

Antimicrobial assessments. Antimicrobial activity of the samples was tested using a modified Kirby-Bauer disc diffusion method [47]. Briefly, 100 μL of the best bacteria/fungi were grown in 10 mL of fresh media until they reached a count of approximately 108 cells/mL for bacteria or 105 cells/mL for fungi [48]. 100 μL of microbial suspension was spread onto agar plates corresponding to the broth in which they were maintained. Isolated colonies of each organism that might be playing a pathogenic role should be selected from primary agar plates and tested for susceptibility by disc diffusion method [49, 50]. Of the many media available, National Committee for Clinical Laboratory Standards (NCCLS) recommends Mueller-Hinton agar. Disc diffusion method for filamentous fungi was the approved standard method (M38-A) developed by the NCCLS [51] for evaluating the susceptibility of filamentous fungi to antifungal agents. Disc diffusion method for yeast was developed as standard method (M44-P) by the NCCLS [52]. Agar-based methods such as Etest disk diffusion can be good alternatives because they are simpler and faster than broth methods [53, 54].

Anti-cancer activity. Human colon carcinoma (HCT-116) cells and human hepatocellular carcinoma (HepG-2) cells were obtained from the American type culture collection ATCC (Rockvill, MD). The cells were grown on RPMI-1640 medium supplemented with 10% inactivated fetal calf serum and 50 μg/mL gentamycin. The cells were maintained at 37ºC in the humidified atmosphere with 5% CO_2 and subcultured two to three times a weak. Monolayers of 10000 cells adhered at the bottom of the wells in a 96-well micro titer plate incubated for 24 h at 37ºC in a humidified incubator with 5% CO_2. The monolayers were then washed with sterile phosphate buffered saline (0.01 M, pH = 7.2) and simultaneously treated with 100 μL the test samples of different dilutions in fresh maintenance medium and incubated at 37ºC. Six wells were used for each concentration of the test samples. Every 24 h the cells were monitored under the inverted microscope. Number of the surviving cells was determined by staining the cells with crystal violet [55, 56] followed by cell lysing using 33% glacial acetic acid and reading the absorbance at 490 nm using ELISA reader (Sun Rise, TECAN, Inc, USA) upon efficient mixing. Absorbance values of untreated cells were considered as 100% proliferation. The number of viable cells was determined using ELISA reader as above and percentage of viability was calculated as $[1 - (OD_t/OD_c)] \times 100\%$, where OD_t is the mean optical density of wells treated with the test sample and OD_c is the mean optical density of untreated cells. 50% inhibitory concentration (IC_{50}) was estimated from graphic plots.

RESULTS AND DISCUSSION

Physical properties. Physical properties and analytical data of albendazole ligand and its Ca(II), Zn(II), Pt(II), Pd(II), and Au(III) complexes are

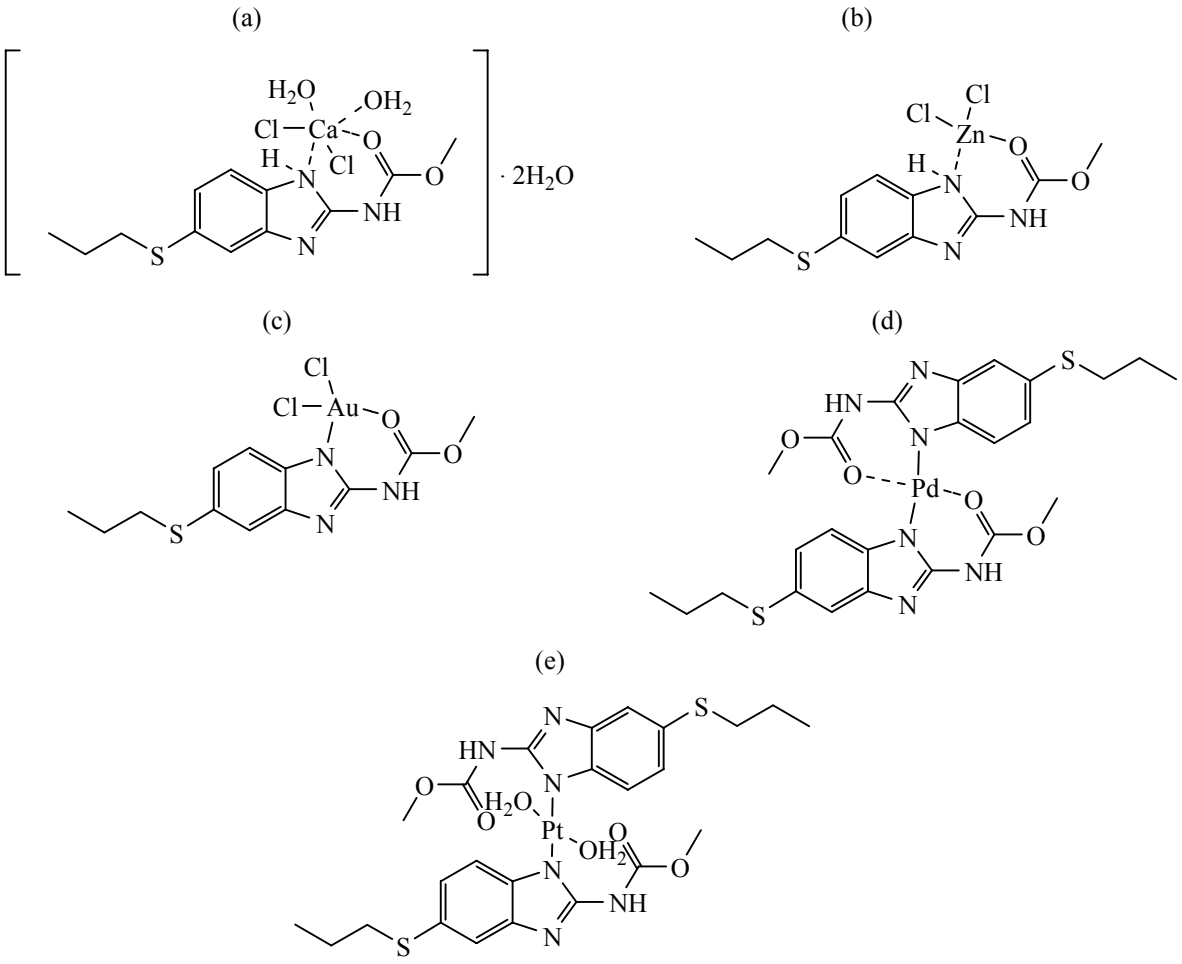

Fig. 2. Suggested formula of (a) $[Ca^{II}(Alb)^{0}(Cl)_2(H_2O)_2]$, (b) $[Zn^{II}(Alb)^{0}(Cl)_2]$, (c) $[Pt^{II}(Alb)_2^{2-}(H_2O)_2]$, (d) $[Pd^{II}(Alb)_2^{2-}]$, and (e) $[Au^{III}(Alb)^{-}(Cl)_2]$ complexes.

presented in Table 1. The isolated complexes were stable in the air and insoluble in H_2O and most organic solvents except DMSO and DMF. Coordination of albendazole towards metal ions was scrutinized by IR, Raman and ^1H NMR spectroscopy, thermal analyses and molar conductance. Elemental analysis of the complexes indicated 1 : 1 or 1 : 2 (metal:ligand) stoichiometry for Ca(II), Zn(II), Au(III), and Pd(II) complexes respectively. Magnetic moments of all diamagnetic al-bendazole complexes were measured at room tem-perature. Low molar conductance values of the complexes revealed their non-electrolytic nature [57], which indicated absence or presence of the conjugated anion covalently attached to the central metal ion. The collected data were in good agreement with the suggested formulas (Fig. 2): $[Ca^{II}(Alb)^{0}(Cl)_2\cdot(H_2O)_2]$, $[Zn^{II}(Alb)^{0}(Cl)_2]$, $[Pt^{II}(Alb)_2^{2-}(H_2O)_2]$, $[Pd^{II}(Alb)_2^{2-}]$, and $[Au^{III}(Alb)^{-}(Cl)_2]$.

IR and Raman spectra (Table 2). Albendazole spectra demonstrated bands of three essential groups: carbamate, benzimidazole, and propylthio.

Intermolecular H-bonding of –NH (Alb) was indicated by the band at 3300 cm^{-1} [58–61] and –NH stretching vibration of N-aryl secondary carbamate was recorded at 3333 cm^{-1}. Stretching vibration band of the H-bonded carbonyl group is shifted to lower value of 1690 cm^{-1} [59–62]. The amide IV band was originated due to coupling between C–N and C–O stretching vibrations. Due to close proximity of the C–S bond to the aromatic system its stretching vibration band was recorded at 603 cm^{-1}.

The mode of chelation was recognized by comparison of free Alb ligand and its complexes. According to IR spectra coordination of the ligand was of neutral bidentate nature and took place via oxygen

Table 2. IR and Raman spectra bands of albendazole free ligand and its metal complexes

Compounds						Group	Assignments
Alb	Ca(II)	Zn(II)	Pt(II)	Pd(II)	Au(III)		
3333 s	3346 br	3329 w	– 3340 m	–	–		ν(NH) ν(OH); H_2O
1712 m	1711 w	1745 vs	1713 m	1713 w	1745 m		ν(C=O); amide I [62]
1524	1524	1540	1525	1526	1529	Carbamate group	ν(CNH); amide II
1272	1272	1242	1272	1273	1254		Amide III
1227	1228	–	1227	1228	–		Amide IV
1100	1100	1102	1100	1100	1096		ν(CO) + ν(CS)
2959 2925 2866	2959 2925 2866	2961 2871	2959 2925 2866	2959 2926 2867	3137 3046 2961 2870	Propyl-S group	ν_{as}(CH); CH_2 +CH_3 ν_s(CH); CH_2 +CH_3
1449 1327	1449 1328	1453 1326	1450 1327	1450 1327	1452 1407		CH_2 deformation
603	604	600	604	603	608		ν(C–S)
1634	1632	1632	1634	1634	1683		ν(C=C); aromatic
1590	1590	1585	1590	1590	1591		ν(C=N)
–	660	660	696	698	698	Benzimidazole	ν(M–O); Raman
–	514	514	513	514	512		ν(M–N); Raman
–	375 360	341 320	–	–	375 346		ν(M–Cl); Raman

of the carbonyl group and nitrogen atom of –NH (benzimidazole). No shift of ν(C=N) and ν(C–S) recorded for Ca(II) and Zn(II) complexes indicated no participation of the groups in complexation. The Raman spectra bands at 660, 514, and 375–260 cm^{-1} (Table 2) indicated the coordination sites. Coordinated and uncoordinated water of Ca(II) and Pt(II) complexes was recorded by broad bands that overlapped with the bands of –NH and C=C stretching vibrations. Coordinated water molecules bands recorded within the region 700–550 cm^{-1} were assigned to different bending motions δ_r, δ_w, and δ_t [59, 60].

The strong NH band of Alb at 3333 cm^{-1} was not found in the spectra of its Au(III) and Pd(II) complexes which indicated deprotonation of the –NH group of benzimidazole. The IR spectra revealed bidentate coordination of the ligand via oxygen of the carbonyl group and nitrogen of –NH (benzimidazole upon deprotonation).

The broad band at 3340 cm^{-1} in IR spectrum of Pt(II) complex was attribute to ν(O–H) of coordinated water. The free ligand carbonyl group band (1712 cm^{-1}) was recorded also in the spectrum of $[Pt^{II}(Alb)_2^{2-}(H_2O)_2]$ indicating that oxygen of the group was not involved in coordination with the central Pt(II) ion. So, ligation of albendazole towards Pt(II) took place via nitrogen atoms of its two deprotonated molecules (Fig. 2).

Magnetic moments and electronic spectra. Magnetic moments of all albendazole complexes calculated from the corrected magnetic susceptibilities determined at room temperature indicated their diamagnetic nature (Table 3). Pd(II), Pt(II), and Au(III) complexes were characterized by the diamagnetic nature and square planar environment around the central metal ions [63, 64]. Electronic spectra of complexes (Table 3) supported their low-spin square planar configuration [65].

Table 3. Electronic spectral bands and magnetic moments of albendazole free ligand and its complexes

Complex	μ_{eff}	Electronic bands, nm	Geometry
Pt(II)	0.12 (diamagnetic)	278, 314	Square planar
Pd(II)	0.26 (diamagnetic)	278, 340, 384	Square planar
Au(III)	0.34 (diamagnetic)	318, 364, 386, 512	Square planar

Table 4. Thermogravimetric data of albendazole complexes

Complex	Steps	DTA peak, °C	DTG peak, °C	Assignments	Weight loss, % found (calculated)
Ca(II)	1 2 Residue	200 455	60, 140, 205 310, 520, 590, 660	$2H_2O + Cl_2$ Albendazole CaO	23.30 (23.86) 63.69 (63.64) 13.01 (12.50)
Zn(II)	1 2 Residue	115 170, 255, 340, 600	115 170, 250, 350, 600	Propyl-S Cl_2 + Albendazole ZnO	17.58 (18.67) 60.66 (61.08) 20.94 (20.25)
Pt(II)	1 2 Residue	78 250, 360, 570	80 180, 280, 335, 570	$2H_2O$ 2Albendazole Pt metal	5.10 (4.74) 69.68 (69.84) 25.22 (25.68)
Pd(II)	1 Residue	350, 440	220, 350, 440	2Albendazole PdO	81.41 (81.04) 18.59 (19.28)
Au(III)	1 Residue	100, 260, 420, 490	120, 270, 410, 490	Cl_2 + Albendazole Au metal	63.20 (63.01) 36.80 (37.01)

^{1}H and ^{13}C NMR spectra (see Scheme 1). *$[Ca^{II}(Alb)^0 \cdot (Cl)_2(H_2O)_2] \cdot 2H_2O$ complex.* ^{1}H NMR (DMSO-d_6), δ, ppm: 0.96 s (3H, CH_3); 1.55 m, 2.86 m (4H, $2CH_2$); 3.37 s (2H, H_2O); 3.75 s (3H, CH_3-COO); 7.08–7.42 m (3H, Ar-H); 4.60 s (1H, NH benzimidazole). *$[Zn^{II}(Alb)^0(Cl)_2]$ complex.* ^{1}H NMR (DMSO-d_6), δ, ppm: 0.96(s, 3H, CH_3); 1.55 m, 2.85 m (4H, $2CH_2$); 3.72 s (3H, CH_3-COO); 7.08–7.41 m (3H, Ar-H); 4.60 s (1H, NH benzimidazole). *$[Pd^{II}(Alb)_2^{2-}]$ complex.* ^{1}H NMR (DMSO-d_6), δ, ppm: 0.96 s (3H, CH_3); 1.56 m, 2.87 m (4H, $2CH_2$); 3.75 s (3H, CH_3-COO); 7.09–7.42 m (3H, Ar-H). Absence of a singlet at 5.00 s (1H, NH benzimidazole ring) was due to deprotonation of –NH confirmed the coordination mode of albendazole toward Pd(II) ions. *$[Au^{III}(Alb)^-(Cl)_2]$ complex.* ^{1}H NMR (DMSO-d_6), δ, ppm: 0.96 s (3H, CH_3); 1.58 m, 2.91 m (4H, $2CH_2$); 3.81 s (3H, CH_3-COO); 7.17–7.73 m (3H, Ar-H). Absence of a singlet at 5.00 s (1H, NH benzimidazole ring) was due to deprotonation of –NH and confirmed the coordination mode of albendazole toward Au(III) ions.

Scheme 1. ^{1}H and ^{13}C NMR data of Alb, δ (ppm).

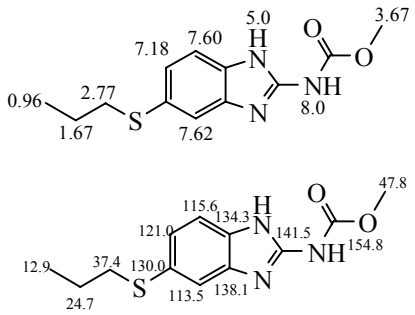

Thermal analyses. TGA data are presented in Table 4. The hydrated complexes demonstrated loss of hydrated and coordinated water molecules in the first and second decomposition stages. Kinetic thermodynamic parameters are shown in Table 5.

In this study we used the integral method of Coats–Redfern [66] to evaluate the kinetic parameters and studied thermal behavior of complexes using the following equations:

$$\ln\left[\frac{1-(1-\alpha)^{1-n}}{(1-n)T^2}\right] = \ln\left(\frac{AR}{\varphi E}\right) - \frac{E}{RT}, \text{ for } n \neq 1, \quad (4)$$

$$\ln\left[\frac{1-(1-\alpha)}{T^2}\right] = \ln\left(\frac{AR}{\varphi E}\right) - \frac{E}{RT}, \text{ for } n = 1, \quad (5)$$

Table 5. Kinetic parameters based on the Coats–Redfern equation for the albendazole complexes

Complex	DTG_{max}, °C	Steps	Thermodynamic parameters	
			parameters	values
Ca(II)	140		E, kJ/mol	110
			A, s^{-1}	3.30×10^{12}
		2	ΔS, J mol^{-1} K^{-1}	–82
			ΔH, kJ/mol	108
			ΔG, kJ/mol	114
			r	0.9986
Zn(II)	170		E, kJ/mol	103
			A, s^{-1}	7.00×10^{11}
		2	ΔS, J mol^{-1} K^{-1}	–21
			ΔH, kJ/mol	99
			ΔG, kJ/mol	105
			r	0.9965
Pt(II)	180		E, kJ/mol	128
			A, s^{-1}	1.70×10^{13}
		2	ΔS, J mol^{-1} K^{-1}	–52
			ΔH, kJ/mol	125
			ΔG, kJ/mol	122
			r	0.9960
Pd(II)	220		E, kJ/mol	80
			A, s^{-1}	2.80×10^{5}
		2	ΔS, J mol^{-1} K^{-1}	–126
			ΔH, kJ/mol	76
			ΔG, kJ/mol	138
			r	0.9950
Au(III)	270		E, kJ/mol	116
			A, s^{-1}	170×10^{9}
		2	ΔS, J mol^{-1} K^{-1}	–75
			ΔH, kJ/mol	112
			ΔG, kJ/mol	150
			r	0.9920

where A is the pre-exponential factor. The correlation coefficient, r, was computed using the least square method for different values of n by plotting the left hand side of Eqs. (4) or (5) versus $1000/T$ [66]. The n value which gave the best fit ($r \approx 1$) was chosen as the order parameter for the decomposition stage of interest. From the intercept and linear slop of such stage, A and E values were determined.

The following remarks can be pointed out:

– All complexes decomposition stages demonstrated best fit for (n =1) indicating the first order decomposition stages in all cases.

– The value of ΔG increased significantly for the subsequent decomposition stages of a given complex due to significant increase of $T\Delta S$ values from one stage to another that were higher than the values of ΔH [67, 68].

– The negative values of activation entropies ΔS indicated the more ordered activation complex than the reactants that slowed down the reactions [69].

Table 6. Crystals sizes (D), dislocation density (δ), and strain (ε) of the complexes

Complex	D, nm	$\delta \times 10^{12}$, lin m^{-2}	$\varepsilon \times 10^{-4}$
$[Pd^{II}(Alb)_2^{2-}]$	4.86	0.042	0.315
$[Au^{III}(Alb)^{-}(Cl)_2]$	5.17	0.037	0.074

Table 7. Quantum chemical parameters of albendazole and $[Ca^{II}(Alb)^0(Cl)_2(H_2O)_2]$, $[Pt^{II}(Alb)_2^{2-}(H_2O)_2]$, and $[Au^{III}(Alb)^{-}(Cl)_2]$

Parameters	Albendazole	Ca(II)	Pt(II)	Au(III)
E_{LUMO}	–4.36	–4.77	–5.01	–4.22
E_{HOMO}	–5.99	–6.65	–6.94	–6.02
ΔE	1.63	1.88	1.93	1.80
χ	5.17	5.71	5.97	5.12
η	0.81	0.94	0.96	0.90
σ	1.23	1.06	1.04	1.11
P_i	–5.17	–5.71	–5.97	–5.12
S	0.61	0.53	0.52	0.55
ω	16.40	17.34	18.47	14.56
ΔN_{max}	6.38	6.07	6.22	5.69

X-ray powder diffraction, SEM and TEM studies. Crystallization for Pd(II) and Au(III) complexes was calculated from the major diffraction patterns of the respective complex using the Debye–Scherrer formula [70]. Their grain size was calculated to be 5.0 nm [71, 72] (Table 6).

According to SEM images of grinded complexes $[Pd^{II}(Alb)_2^{2-}]$ and $[Au^{III}(Alb)^{-}(Cl)_2]$ (Figs. 3a, 3b) the synthesized products were NPs, that had uniform shape.

According to TEM the diameter of Au(III) complex particles was ca 5 nm. TEM and XRD data for the complex matched well.

Molecular modeling. In the absence of single crystal data for albendazole ligand and its complexes

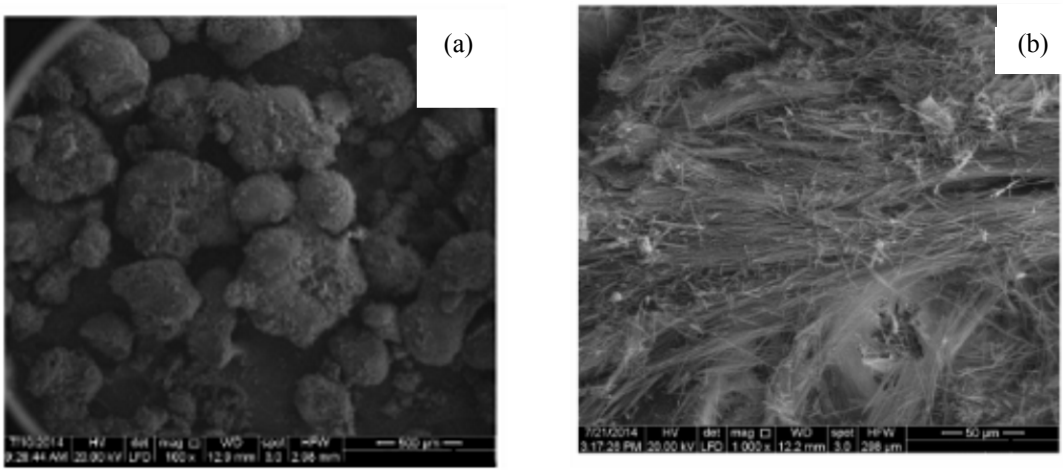

Fig. 3. SEM images of (a) $[Pd^{II}(Alb)_2^{2-}]$ and (b) $[Au^{III}(Alb)^{-}(Cl)_2]$.

quantum chemical calculations and molecular modeling studies were useful in supporting the suggested structures [73, 74]. Geometry optimization and conformational analysis have been performed using semi-empirical PM3 level [74] as implemented in software of Hyperchem 7.5 program [75]. Quantum chemical parameters based on PM3 method and implemented in HyperChem [75–80] are listed in Table 7.

Molecular modelling data (Chem Office Ultra–7) supported the ligation process via the carbamide oxygen and deprotonated benzimidazole nitrogen for Pd(II) and Au(II) and non-deprotonated –NH for Ca(II) and Zn(II). Pt(II) ions coordinated with albendazole ligand entirely via deprotonated benzimidazole ring. Length of $C{=}O_{amide}$ and $-NH_{benzimidazole}$ bonds of free ligand were calculated to be longer in complexes. Length of other bonds and angles values in Alb did not change upon complexation.

All calculations data can be readily provided by the authors upon request.

Table 8. Inhibition zone diameters (mm/mg sample) of albendazole and its complexes against some kinds of bacteria and fungi

Inhibition zone diameter (mm/mg sample)						Sample	
Candida albicans (Fungus)	*Aspergill flavus* (Fungus)	*Staphylococcus aureus* (G^+)	*Pseudomonas aeruginosa* (G^-)	*Escherichia coli* (G^-)	*Bacillus subtilis* (G^+)		
0.0	0.0	0.0	0.0	0.0	0.0	Control: DMSO	
–	–	30	34	32	34	Tetracycline Antibacterial agent	Standard
19	18	–	–	–	–	Amphotericin B Antifungal agent	Standard
14	12	24	12	15	20	Albendazole ligand	
11	5	14	10	12	16	Ca(II)	
15	10	22	28	27	25	Zn(II)	
16	12	19	28	21	25	Pt(II)	
20	11	16	19	16	14	Pd(II)	
26	21	46	42	39	44	Au(III)	

Table 9. Inhibitory activity of Au(III) complex against colon carcinoma and hepatocellular carcinoma cells

Sample concentration, μg	Viability			
	HepG-2 cell line		HCT-116 cell line	
	doxrubcin	Au(III)	doxrubcin	Au(III)
50.00	4.91	6.57	6.82	8.93
25.00	8.87	9.29	8.89	17.07
12.50	14.83	13.98	14.83	28.96
6.25	16.16	19.36	16.16	41.58
3.125	25.28	38.78	22.28	63.76
1.56	34.64	74.53	34.64	81.22
0.78	45.79	79.62	45.78	87.47
0.39	51.08	88.17	51.28	92.35
0.00	100.00	100.00	100.00	100.00
IC_{50}	0.467	2.63	0.471	5.06

Antimicrobial assessments. *In vitro* antibacterial and antifungal assessments of free albendazole and its Ca(II), Zn(II), Pt(II), Pd(II), and Au(III) complexes were tested against Gram(+) bacteria *Staphylococcus Aureus, Bacillus subtilis,* and Gram(–) bacteria *Escherichia Coli*, *Pseudomonas aeruginosa* and fungi as *Candida Albicans* and *Aspergillus flavus* (Table 8). Standard discs of tetracycline (antibacterial agent) and amphotericin B (antifungal agent) were utilized in this study. Au(III) complex demonstrated higher activity than the standards and other complexes probably due to its significant lipophilic character. Low activity of Ca(II) complex was attributed to its low lipid solubility that retarded its penetration through cells membranes [81–83].

Au(III) complex was tested for its anti-cancer activity. *In vitro* cytotoxicity assessment was performed on human colon carcinoma (HCT-116) cell line and human hepatocellular carcinoma (HepG-2) cell line in the presence of doxrubcin standard drug (Table 9). According to the accumulated data Au(III) complex was more efficient for HepG-2 cell line than HCT-116.

REFERENCES

1. Sekhon, B.S., *J. Pharm. Educ. Res*., 2010, vol. 1(1), p. 1.
2. Von Nussbaum, F., Brands, M., Hinzen, B., Weigand, S., and Häbich, D., *Angew. Chem. Int. Ed*., 2006, vol. 45, p. 5072.
3. Ming, L.J., *Med. Res. Rev*., 2003, vol. 23, p. 697.
4. Ming, L.J., *J. Chin. Chem. Soc*., 2010, vol. 57, p. 285.
5. Ajibola, A.O., *Essential of Medicinal Chemistry*, Sharson Jersey, 2nd ed., 1990, pp. 28–446.
6. Obaleye, J.A., Nde-aga, J.B., and Balogun, E.A., *African J. Sci*., 1997, vol. 1, p. 10.
7. Ogunniran, K.O., Tella, A.C., Alensela, M., and Yakubu, M.T., *African J. Biotechnol*., 2007, vol. 10, p. 1202.
8. El-Ajaily, M.M., Abdlseed, F.A., Ben-gweirif, S., *J. Chem*., 2007, vol. 4, p. 461.
9. Sultana, N., Arayne, M.S., *Pak. J. Pharm. Sci*., 2007, vol. 20, p. 305.
10. Arayne, S., Sultana, N., Haroon, U., and Mesaik, A.M., *Bioinorg. Chem. Appl*., 2009, vol. 2009, p. 914105.
11. Jung, H., Medina, L., Garcia, L., Fuentes, I., and Moreno-Esparza, R., *J. Pharm. Pharmacol*., 1998, vol. 50, p. 43.
12. Wen, H., New, R.R.C., and Craig, P.S., *Br. J. Clin. Pharm*., 1993, vol. 35, p. 565.
13. Del-Brutto, O.H. and Sotelo Roman, G.C., *Clin. Infect. Dis*., 1993, vol. 17, p. 730.
14. Nguyen, P.T.M., Baldeck, J.D., Olsson, J., and Marquis, R.E., *Oral Microbiol. Immunol*., 2005, vol. 20, p. 93.
15. Podunavac-Kuzmanović, S.O. and Cvetković, D.D., *Centr. Eur. J. Occupat. Environ. Med*., 2006, vol. 12, p. 55.
16. Podunavac-Kuzmanović, S.O., Leovac, V.M., Perišić-Janjić, N.U., Rogan, J., and Balaž, J., *J. Serb. Chem. Soc*., 1999, vol. 64, p. 381.
17. Podunavac-Kuzmanović, S.O. and Markov, S.L., *Centr. Eur. J. Occupat. Environ. Med*., 2006, vol. 12, p. 61.
18. Podunavac-Kuzmanović, S.O. and Cvetković, D.D., *J. Serb. Chem. Soc*., 75 (2007), p. 459.
19. Ates-Alagoz, Z., Yildiz, S., and Buyukbingol, E., *Chemotherapy*, 2007, vol. 53, p. 110.
20 Ayhan-Kilcigil, G. and Altanlar, N., *Turk. J. Chem*., 2006, vol. 30, p. 223.
21. Mohamed, B.G., Hussein, M.A., Abdel-Alim, A.M., and Hashem, M., *Arch. Pharm. Res*., 2006, vol. 29, p. 26.
22. Kus, C., Ayhan-Kilcigil, G., Can-Eke, B., and Iscan, M., *Arch. Pharm. Res*., 2004, vol. 27, p. 156.
23. Nakano, H., Inoue, T., Kawasaki, N., Miyataka, H., Matsumoto, H., Taguchi, T., Inagaki, N., Nagai, H., and Satoh, T., *Chem. Pharm. Bull*., 1999, vol. 47, p. 1573.
24. Valdez, J., Cedillo, R., Hernandez-Campos, A., Yepez, L., Hernandez-Luis, F., Navarrete-Vazquez, G., Tapia, A.,

Cortes, R., Hernandez, M., and Castillo, R., *Bioorg. Med. Chem. Lett*., 2002, vol. 12, p. 2221.
25. Ward, C., Berthold, R., Koerwer, J., Tomlin, J., and Manning, T., *J. Agric. Food Chem*., 1986, vol. 34, p. 1005.
26. Lipkowitz, K.B. and McCracken, R.O., *Parasitol. Res*., 1993, vol. 79, p. 475.
27. Campbell, W.C., *Parasitol. Today*, 1990, vol. 6, p. 130.
28. Didier, E.S., Stovall, M.E., Green, L.C., Brindley, P.J., Sestak, K., and Didier, P.J., *Vet. Parasitol*., 2004, vol. 126, p. 145.
29. Pandey, V.K., Upadhay, M., Dev Gupta, V., and Tandon, M., *Acta Pharm*., 2005, vol. 55, p. 47.
30. Patel, P.D., Patel, M.R., Kaushik-Basu, N., and Talele, T.T., *J. Chem. Inf. Model*, 2008, vol. 48, p. 42.
31. Arjmand, F., Mohani, B., and Ahmad, S., *Eur. J. Med. Chem*., 2005, vol. 40, p. 1103.
32. Miller, V.L., Gould, C.J., Csonka, E., and Jensen, R.L., *J. Agr. Food Chem*., 1973, vol. 21, p. 931.
33. Singh, V.P. and Katiyar, A., *Pestic. Biochem. Phys*., 2008, vol. 92, p. 8.
34. Saczewski, F., Dziemidowicz-Borys, E., Bednarski, P.J., Grert, R., Gdaniec, M., and Tabin, P., *J. Inorg. Biochem*., 2006, vol. 100, p. 1389.
35. Rodriguez, M.C., Mosquera-Vazquez, S., Sanmartin-Matalobos, J., Garcia-Deibe, A.M., Pelizzi, C., and Zani, F., *Polyhedron*, 2010, vol. 29, p. 864.
36 LopezC–Sandoval, H., Londono-Lemos, M.E., Garza-Velasco, R., Poblano-Melendez, I., Granada-Macias, P., Gracia-Mora, I., and Barba-Behrens, N., *J. Inorg. Biochem*., 2008, vol. 102, p. 1267.
37. Gumus, F., Pamuk, I., Ozden, P., Yildiz, S., Diril, N., Oksuzoglu, E., and Ozkul, A., *J. Inorg. Biochem*., 2003, vol. 94, p. 255.
38. Skalitzky, D.J., Marakovits, J.T., Maegley, K.A., Ekker, A., Yu, X.H., Hostomsky, Z., Webber, S.E., Eastman, B.W., Almassy, R., Li, J., Curtin, N.J., Newell, D.R., Calvert, A.H., Griffin, R.J., and Golding, B.T., *J. Med. Chem*., 2003, vol. 46, p. 213.
39. Hauel, N.H., Nar, H., Prirpke, H., Ries, U., Stassen, J.M., and Wienen, W.J., *J. Med. Chem*., 2002, vol. 45, p. 1757.
40. El-Metwaly, N.M. and Refat, M.S., *Spectrochim. Acta Part A*, 2011, vol. 78, p. 196.
41. Refat, M.S., S.F. Mohamed, *Spectrochim. Acta Part A*, 2011, vol. 82, p. 108.
42. Refat, M.S., *J. Mol. Str*., 2013, vol. 1037, p. 170.
43. Refat, M.S., *Spectrochim. Acta Part A*, 2013, vol. 105, p. 326.
44. El-Megharbel, S.M., Hamza, R.Z., and Refat, M.S., *Spectrochim. Acta Part C*, 2014, vol. 131, p. 534.
45. El-Megharbel, S.M., Hamza, R.Z., and Refat, M.S., *Chem. Biol. Inter.*, 2014, vol. 220, p. 169.
46. Selwood, P.F., *Magnetochemistry*, New York: Wiley, 1956, 2nd ed.
47. Bauer, A.W., Kirby, W.M., Sherris, C., and Turck, M., *Am. J. Clin. Pathology*, 1996, vol. 45, p. 493.
48. Pfaller, M.A., Burmeister, L., Bartlett, M.A., and Rinaldi, M.G., *J. Clin. Microbiol*., 1988, vol. 26, p. 1437.
49. *National Committee for Clinical Laboratory Standards*, *Performance Volume. Antimicrobial Ausceptibility of Flavobacteria*, 1997.
50. *National Committee for Clinical Laboratory Standards. Methods for Dilution Antimicrobial Susceptibility Tests for Bacteria That Grow Aerobically. Approved Standard M7-A3,* Villanova, Pa, 1993.
51. *National Committee for Clinical Laboratory Standards. Reference Method for Broth Dilution Antifungal Susceptibility Testing of Conidium-Forming Filamentous Fungi: Proposed Standard M38-A*, NCCLS, Wayne, PA, USA, 2002.
52. *National Committee for Clinical Laboratory Standards. Methods for Antifungal Disk Diffusion Susceptibility Testing of Yeast: Proposed Guideline M44-P*, NCCLS, Wayne, PA, USA, 2003.
53. Liebowitz, L.D., Ashbee, H.R., Evans, E.G.V., Chong, Y., Mallatova, N., and Zaidi, M., *Diagn. Microbiol. Infect. Dis*., 2001, vol. 4, p. 27.
54. Matar, M.J., Ostrosky-Zeichner, L., Paetznick, V.L., Rodriguez, J.R., Chen, E., and Rex, J.H., *Antimicrob. Agents Chemother*., 2003, vol. 47, p. 1647.
55. Mosmann, T., *J. Immunol. Methods*, 1983, vol. 55, p. 65.
56. Gangadevi, V. and Muthumary, J., *African J. Biotechnol.*, 2007, vol. 6, p. 1382.
57. Geary, W.J., *Coord. Chem*., 1971, vol. 7, p. 81.
58. Socrates, G., *Infrared Characteristic Group Frequencies*, New York: Wiley, 1980.
59. Nakamoto, K., *Infrared Spectra of Inorganic and Coordination Compounds*, New York: Wiley, 1970, 2nd ed.
60. Bellamy, L.J., *The Infrared Spectra of Complex Molecules*, London: Chapman and Hall, 1975.
61. Gunasekaran, S. and Uthra, D., *Asian J. Chem*., 2008, vol. 20(8), p. 6310.
62. Dubey, P.K., Naidu, A., Anandam, V., and Hemasunder, G., *Indian J. Chem B*., 2005, vol. 44, p. 1239.
63. Amin, O.H., Al-Hayaly, L.J., Al-Jibori, S.A., and Al-Allaf, T.A.K., *Polyhedron*, 2004, vol. 23, p. 2020.
64. Abdalrazaq, E.A., Buttrus, N.H., and Abd Al-Rahman, A.A., *Asian J. Chem*., 2010, vol. 22(3), p. 2179.
65. Tunney, J.M., Blake, A.J., Davies, E.S., Mcmater, J., Wilson, C., and Garner, C.D., *Polyhedron*, 2006, vol. 25(2), p. 591.
66. Coats, A.W. and Redfern, J.P., *Nature*, 1964, vol. 201, p. 68
67. Maravalli, P.B. and Goudar, T.R., *Thermochim Acta,*

1999, vol. 325, p. 35.

68. Yusuff, K.K.M. and Sreekala, R., *Thermochim Acta,* 1990, vol. 159, p. 357.
69. Frost, A.A. and Peasron, R.G., *Kinetics and Mechanism*, New York: Wiley, 1961.
70. Cullity, B.D., *Elements of X-Ray Diffraction*, Addison-Wesley, Reading, MA, 1972, p. 102.
71. Salavati-Niasari, M., Mohandes, F., Davar, F., Mazaheri, M., Monemzadeh, M., and Yavarinia, N., *Inorg. Chim. Acta*, 2009, vol. 362(10), p. 3691.
72. Velumani, S., Mathew, X., and Sebastian, P.J., *Solar Energy Mater. Solar Cells*, 2003, vol. 76, p. 359.
73. Yousef, T.A., Abu El-Reash, G.M., and El Morshedy, R.M., *J. Mol. Struct*., 2013, vol. 1045, p. 145.
74. Helal, M.H., El-Awdan, S.A., Salem, M.A., Abd-elaziz, T.A., Moahamed, Y.A., ElC–Sherif, A.A., and Mohamed, G.A.M., *Spectrochim. Acta Part A*, 2015, vol. 135, p. 764.
75. *Hyper Chem. Version 7.51 Hyper cube*, INC.
76. Pearson, R.G., *J. Org. Chem*.,1989, vol. 54, p. 1423.
77. Geerlings, P., De Proft, F., and Langenaeker, W., *Chem. Rev*., 2003, vol. 103, p. 1793.
78. Parr, R.G., *J. Am. Chem. Soc*., 1999, vol. 121, p. 1922.
79. Chattaraj, P.K. and Giri, S., *J. Phys. Chem. A*, 2007, vol. 111, p. 11116.
80. Speie, G., Csihony, J., Whalen, A.M., and Pie-Pont, C.G., *Inorg. Chem*., 1996, vol. 35, p. 3519.
81. Khatiwora, E., Joshi, P., Puranik, V.G., Darmadhikari, D., Athawale, A., Deshpande, N.R., and Kashalkar, N.R., *Int. J. Chem. Sci*., 2013, vol. 11(1), p. 12.
82. Frobisher, M., Hinsdill, R.D., Crabtree, K.T., and Goodheart, C.R., *Fundamentals of Microbiology*, Toppan Company Ltd., 1974, 9th ed., p. 328.
83. Raman, N., Kulandaisamy, A., and Thangaraja, C., *Trans. Metal Chem*., 2004, vol. 29, p. 129.